NASA TECHNICAL NOTE

NASA TN D-3206

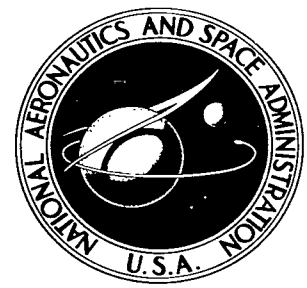

NASA TN D-3206

INVESTIGATION OF BONDED PLASTIC TAPE FOR LINING FILAMENT-WOUND FIBER-GLASS CRYOGENIC PROPELLANT TANKS

by Robert W. Frischmuth, Jr., and Paul T. Hacker

Lewis Research Center
Cleveland, Ohio

NATIONAL AERONAUTICS AND SPACE ADMINISTRATION • WASHINGTON, D. C. • JANUARY 1966

NASA TN D-3206

INVESTIGATION OF BONDED PLASTIC TAPE FOR LINING FILAMENT-WOUND FIBER-GLASS CRYOGENIC PROPELLANT TANKS

By Robert W. Frischmuth, Jr., and Paul T. Hacker

Lewis Research Center
Cleveland, Ohio

NATIONAL AERONAUTICS AND SPACE ADMINISTRATION

For sale by the Clearinghouse for Federal Scientific and Technical Information
Springfield, Virginia 22151 – Price $2.00

INVESTIGATION OF BONDED PLASTIC TAPE FOR LINING FILAMENT-WOUND FIBER-GLASS CRYOGENIC PROPELLANT TANKS

by Robert W. Frischmuth, Jr. and Paul T. Hacker

Lewis Research Center

SUMMARY

The use of filament-wound fiber-glass liquid-hydrogen propellant tank structures should result in a considerable weight savings compared to conventional metal tanks providing that a suitable internal liner can be developed. This report investigates the use of plastic tape liners bonded to the inner surface of the filament-wound structure. The compatibility of liners, made of Teflon and Mylar tape, with respect to the filament-wound shell was studied experimentally using liquid hydrogen and theoretically using an analytical technique derived in this report. The investigation shows for bonded liners used at the temperature of liquid hydrogen (normal boiling point 20° K) that Teflon is incompatible with the filament-wound structure and Mylar is limited; upon tank pressurization, the Mylar liner will fail in tension before the burst pressure of the filament-wound structure is approached.

INTRODUCTION

The development of lightweight tank structures for cryogenic propellants is a necessary objective, if the efficiency of rocket propulsion stages is to be increased substantially. Filament-wound fiber-glass reinforced plastic tanks are a potential lightweight structure for this purpose. This type of structure has shown high strength-to-weight ratios in pressure vessels and has been successful as solid rocket motor cases for several years. The utilization of this type of structure for cryogenic liquid propellant tanks for rocket vehicles requires further developmental effort because of the unknown effects of low temperatures on the materials used in the composite structure.

Of primary concern is the tank wall liner required to seal the generally porous resin-impregnated glass filament structure. The characteristically high elongation (3 to 4 percent) of the glass-resin composite walls under pressure requires the liner generally to

be of a material capable of high elastic strain. At normal temperatures this presents no problem but at cryogenic temperatures most elastic materials generally lose their high elongation properties, become brittle and thus unsuitable as liner materials. If the weight advantage of fiber-glass reinforced plastic compared to metals for propellant tanks is to be realized, a lightweight liner useable at liquid-hydrogen temperatures must be developed.

The NASA Lewis Research Center is now conducting an investigation, described in references 1 to 5, to evaluate various methods of lining a fiber-glass tank. Basically there are two possible liner - fiber-glass shell configurations. One is to have the liner separate from the fiber-glass - resin composite shell, that is, free floating. The other approach is to make the liner as an integral part of the tank wall, that is, bonded to the wall. In the case of the free-floating liner, the liner and the fiber-glass shell can be fabricated separately and after completion, the liner can be inserted into the shell. The obvious advantage of this approach is the capability of replacing the liner. Some foreseeable problem areas, however, in this method are: avoidance of damage to the thin materials during handling and obtaining a smooth inner surface of the filament-wound shell. Since the liner is free to move with respect to the shell, rough areas could damage the liner. For the bonded liner case, the interaction of the liner with the filament-wound structure from thermally induced stresses and internal pressure loads presents problems because of differences in physical properties of the various component materials.

Although there are some obvious problems associated with liners there may be others that are not definable under the present state of the technology. In addition, there is a question as to whether the filament-wound fiber-glass reinforced plastic tank structure itself can withstand a limited number of repeated pressure and temperature cycles imposed by a cryogenic liquid, especially liquid hydrogen.

Analytical expressions for predicting the mechanical behavior of composite structures, such as the filament wound tanks, when subjected to combined thermally induced stresses and mechanical loads can be derived if equilibrium conditions and other simplifying assumptions are made. During filling of a filament-wound tank with liquid hydrogen, rapidly decreasing temperatures and steep temperature gradients will be present resulting in nonequilibrium conditions. Thus it is presently necessary to supplement analytical methods and models with experimental data. The difficulty of the problem of predicting the mechanical behavior of a cryogenic filament-wound tank is further accentuated by the lack of data on the thermal and physical properties of materials over the range of temperatures encountered. In order to assess the feasibility of filament-wound tanks for storage of cryogenic propellants and to define specific problem areas, experimental tank fabrication and testing are a necessary part of an overall investigation.

This report presents the results of a preliminary investigation of fiber-glass filament-wound cryogenic tanks using an internal liner made of plastic film in tape form

and bonded to the fiber-glass structure. The objectives of the investigation were to define problem areas, to evaluate the feasibility of a limited number of materials, to develop fabrication techniques especially the bonded liner concept, and to obtain information for establishing and checking the validity of analytical methods. The program consisted of the following sequential steps: (1) design, fabrication and testing of a small tank with design and materials selection based primarily on the current state of technology, (2) a limited study to determine pertinent property data for possible component materials that become evident in step (1) as being required, and (3) design, fabrication and testing of a second tank of the same size but incorporating changes in design and materials as indicated in the previous steps. A cylindrical tank 18 inches in diameter and 36-inches long was selected in order to utilize existing filament-winding tooling and machines. The first tank was lined with Teflon FEP, while the second was lined with Mylar A. Both tanks used Owens-Corning ECG-150-1/0 HTS Fiberglas rovings. Included in this report are the design and fabrication of the lined test tanks, the test results with liquid hydrogen, some materials property data, and an analysis of the mechanical behavior of filament-wound fiber-glass tanks with bonded liners subjected to thermal stresses and pressure loads.

The design and fabrication of the tanks and the materials properties studies were contracted to and performed by Narmco Research and Development Division of Telecomputing Corporation for NASA, Lewis Research Center. Analysis and testing of the tanks with liquid hydrogen and evaluation of results were made by NASA personnel at Lewis Research Center.

SYMBOLS

A cross-sectional area of glass in one strand, sq in./strand

C a constant, $\frac{E_L t_L}{(1 - \nu^2)E_g A}$, in.$^{-1}$

D strand density, strands/in. measured perpendicular to strand direction

E modulus of elasticity, lb/sq in.

F_o initial filament winding tension, lb/strand

K_1 $\sum_i D_i \sin^4 \alpha_i$, strands/in.

K_2 $\sum_i D_i \sin^2\alpha_i \cos^2\alpha_i$, strands/in.

K_3 $\sum_i D_i \cos^4\alpha_i$, strands/in.

N load, lb/in.

P pressure, lb/sq in.

r tank radius, in.

S thermal contraction, in./in.

t thickness, in.

α filament winding angle, see fig. 5, deg

ϵ strain, in./in.

ϵ^F strain due to winding shell under tension, in./in.

$\epsilon(P)$ tank strain due to pressure, in./in.

ϵ^T strain due to thermally induced stresses, in./in.

ν Poisson's ratio of the liner material at -423° F

Subscripts:

g glass fiber only at -423° F

g, RT glass fiber only at room temperature

i refers to a filament wrap all at the same α

L liner

max maximum

S fiber-glass shell

ult uniaxial ultimate for the liner material at -423° F

Z axial (longitudinal) direction, see fig. 5

θ circumferential direction, see fig. 5

DESCRIPTION OF TWO EXPERIMENTAL TANKS

The contractor was provided with the following specifications for the fabrication of the two experimental tanks:

(1) The structural shell was to be made of fiber-glass reinforced plastics using the filament-winding technique.

(2) The structural shell was to be provided with an internal-bonded liner capable of holding liquid and gaseous hydrogen and be mechanically compatible with the shell wall over a temperature range from 520° to -423° F.

(3) A maximum working pressure of 75 pounds per square inch gage was specified for the first tank. The first tank was built to this specification but other structural requirements resulted in an unbalanced design (filaments in circumferential and longitudinal windings not loaded equally when tank is pressurized). Thus for the second tank the maximum pressure was increased to 775 pounds per square inch gage in order to produce a tank of balanced design.

(4) The tanks were to have minimum weight consistent with structural requirements.

(5) The tanks were to have a fill port with filling at one end with the other end closed by the longitudinal filament windings.

(6) They were to be designed to operate in a typical cryogenic propellant tank environment which consisted of the following:

(a) Fabricated, pressure checked, and stored at room temperature

(b) Cold shocked by filling with liquid nitrogen at atmospheric pressure followed by a pressure check at room temperature

(c) Cold shocked by filling with liquid hydrogen at atmospheric pressure followed by a pressure check at room temperature

(d) Filled with liquid hydrogen and slowly pressurized to working pressure

(e) Pressure cycled several times with liquid hydrogen

A specific size and shape of tank was not required, therefore the size and configuration was selected on the basis of existing tooling and manufacturing processes for filament-wound tank structures. The contractor possessed the necessary tooling and filament-winding machinery to produce a cylindrical tank 18 inches in diameter and 36 inches in overall length, so this size was selected. For the tank liner, the contractor's proposal to use a plastic material in tape form which would be applied along with an adhesive to the mandrel by a filament-winding machine prior to the fiber-glass shell, was adopted. Selection of materials and design was left to the contractor.

Table I, and figures 1 and 2 describe the design of the two tanks. Both have liners made up of four layers of overlapping 1-inch-wide by 0.002-inch-thick tape. Teflon was used in tank 1 and Mylar in tank 2. The liner adhesive and shell resin were the same for both tanks, Narmco X-292. The glass fiber used was also the same, Owens-Corning E-HTS. The filament-winding patterns used in the structural shells of the two vessels were quite different. The shell of tank 1 was of relatively light construction composed of longitudinal and circumferential wraps (shown in fig. 1). The density of longitudinal filaments in the dome section of tank 1 required for an internal pressure of 75 pounds per

TABLE I. - MATERIALS AND FABRICATION OF TWO TEST TANKS

	Tank 1		Tank 2		
Liner	Four layers of overlapping 1-in.-wide Teflon tape		Four layers of overlapping 1-in.-wide Mylar tape		
Shell resin and liner adhesive	Narmco X-292		Narmco X-292		
Fiber glass	Owens-Corning E-HTS		Owens-Corning E-HTS		
Fiber-glass pretension	Negligible		1 lb/strand		
Wrap pattern	Longitudinal	Circumferential	Longitudinal	Circumferential	Helical
Winding angle,[a] α, deg[a]	[b]4^{o} 50'	90^{o}	[b]4^{o} 50'	90^{o}	60^{o}
Strands per inch of circumference, D_z	668	0	668	0	358
Strands per inch measured perpendicular to strand direction, D	670	300	670	715	715
Shell thickness,[c] in.	0.040		0.088		
Liner thickness,[c] in.	0.0133		0.0133		

[a]Angle between strand direction and longitudinal axis of tank. Filaments in a particular wrap are actually divided between the angle and its negative.

[b]Average.

[c]Cylindrical portion of tank.

square inch gage was not sufficient to support the liner. Therefore additional longitudinal strands had to be applied (a strand is a bundle of 204 individual filaments). This lead to a highly unbalanced shell design. A balanced design tank is one in which all fillaments are under uniform tension with application of internal pressure. A minimum weight shell is of nearly balanced design (often a slight imbalance is used since experience has shown that the filament efficiency, ratio of developed filament stress to basic filament strength, is not quite as high for longitudinal windings as for circumferential windings). Tank 2 was of heavier construction composed of longitudinal, circumferential, and helical wraps (shown in fig. 2, p 7). The glass strands in tank 2 were pretensioned during the filament winding processes in an attempt to increase the available liner strain.

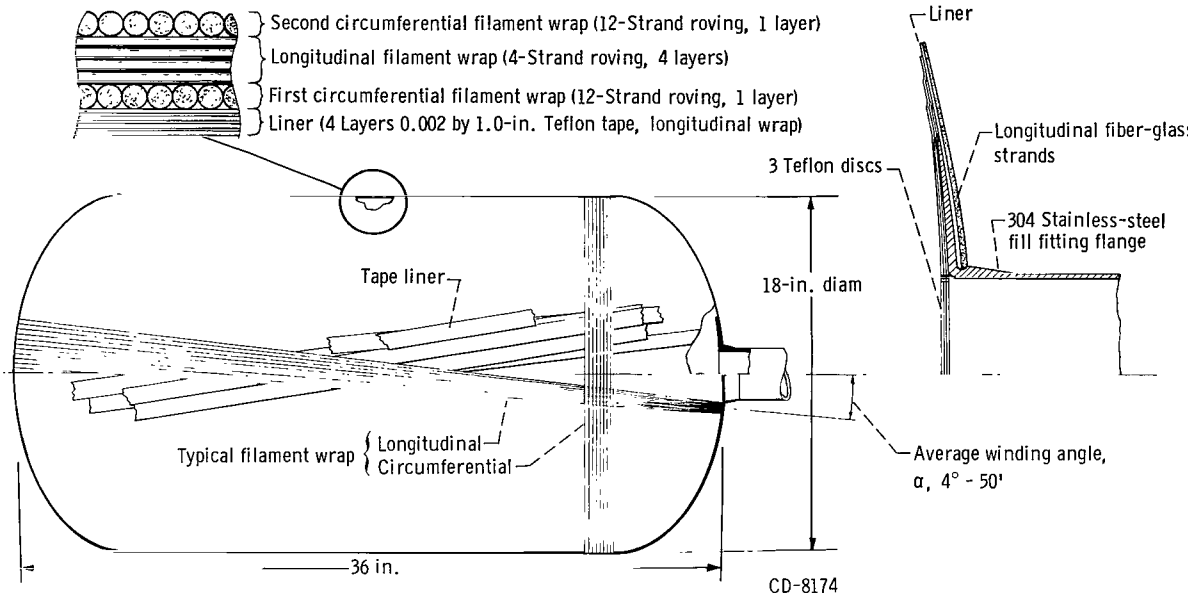

Figure 1. - Schematic of tank 1 with bonded Teflon tape liner.

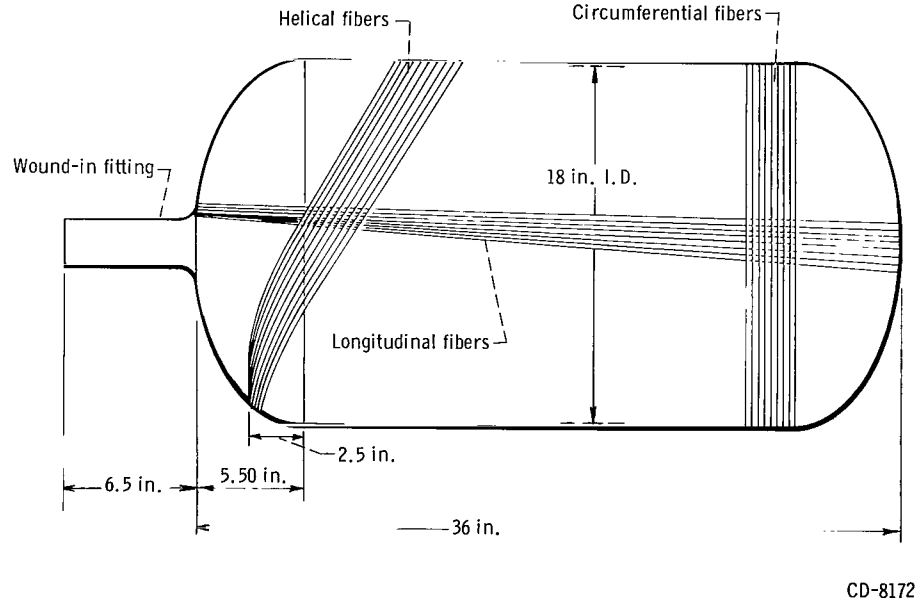

Figure 2. - Schematic of tank 2 (Mylar tape liner) with additional helical wrap.

As previously mentioned this program involves (1) making and testing a tank (tank 1) based on the state of the art materials data, (2) a limited materials study, and (3) making and testing another tank (tank 2) based on the knowledge gained from the materials study. It was anticipated that tank 1 might not perform completely satisfactorily since it was designed and fabricated before the materials study. Its primary purpose was to point out problems associated with the bonded liner configuration and show what properties should be measured in the materials study program. The data obtained in the materials study is presented in appendix A.

TEST FACILITY AND PROCEDURE

The main objective of the experimental testing was to determine the effect of liquid-hydrogen temperature (-423^{o} F) on the structural integrity of the tanks. The low temperature compatability of the bonded plastic tape liners with the fiber-glass shell was of major interest. In general the facility, instrumentation and procedure used in testing the two experimental tanks were the same. Some additional instrumentation was used in testing the second tank.

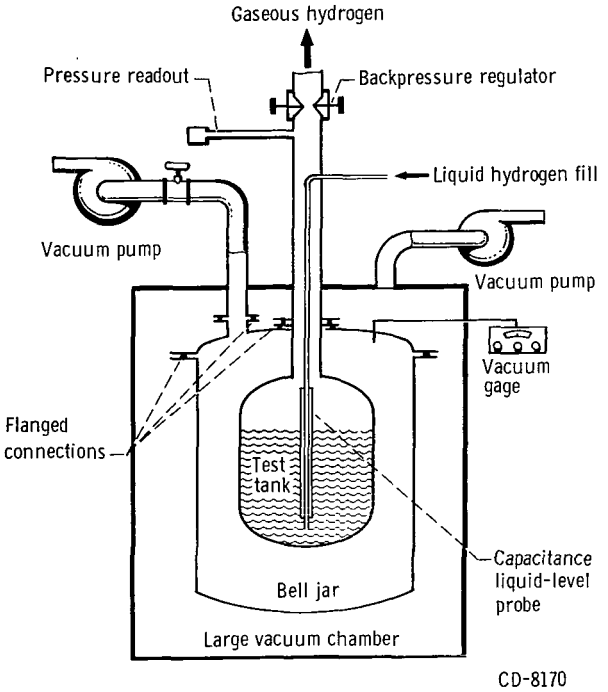

Figure 3. - Liquid-hydrogen test facility.

Facility

The facility used to test the experimental tanks is shown schematically in figure 3. The facility consists basically of two vacuum tanks one inside the other, two vacuum pumping systems, and the cryogenic fluid flow system (fill and vent lines). The test tank was mounted in the bell jar (inside vacuum tank) which served a dual purpose. First, the vacuum in the bell jar insulates the tank so that it can be filled with liquid hydrogen and kept full for a reasonable length of time. Second, the bell jar provides a fixed known volume so that the leak rate of the test tank could be determined by the rate of change of pressure in the bell jar. A major problem associated with the determination of leak

rate by measuring pressure rise in a control volume is the elimination of extraneous leaks into the volume. For the evacuated bell jar, the problem of sealing it against leak from the outside was made difficult because low temperature vacuum seals were required. This problem was overcome by placing the bell jar within another vacuum chamber. This arrangement removed the pressure driving force across the seals and thereby eliminated the extraneous leaks.

The instrumentation that was common for tests of the two experimental tanks shown in figure 3 consisted of the following:

(1) A pressure transducer of the strain-gage type used for measuring internal pressure of test tank

(2) A capacitance-type liquid-level probe for measuring contents of test tank

(3) A hot-filament type vacuum gage to measure pressure in bell jar for determination of leak rate. The vacuum measurement was recorded on a strip chart.

For the second experimental tank, some additional tank instrumentation was used. Thermocouples were placed at various locations (fig. 4) on the outer surface of the tank to measure the structure temperature during cooldown. The copper-constantan thermocouples were secured to the filament-wound structure by an adhesive. A strain gage (fig. 4) was also used to measure the average circumferential tank strain for various tank pressures and temperatures. The gage consists of a stainless-steel band, backed with a dry lubricant (Teflon tape) that fits around the tank. The band is spring loaded through a sissors-type lever system to keep the band taut around the tank. As the tank expands the motion is multiplied in the lever system and transferred to a linear potenti-

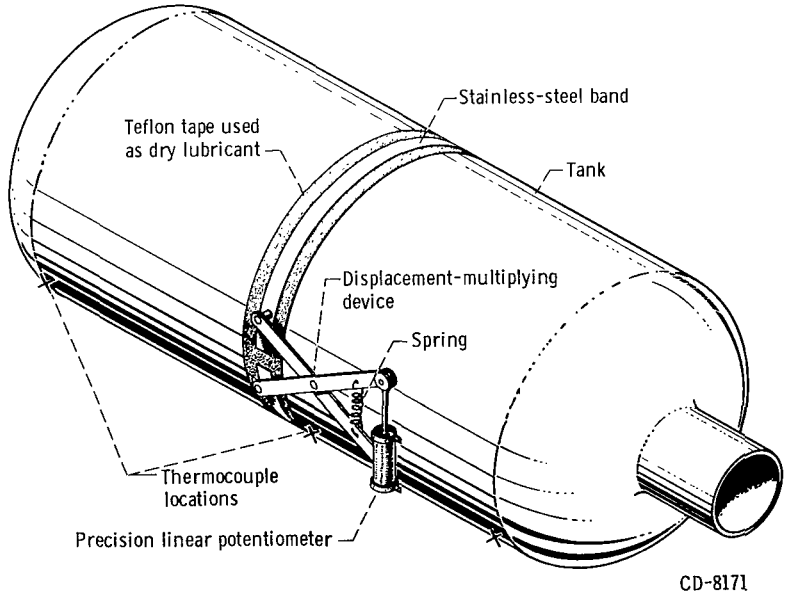

Figure 4. - Additional instrumentation for tank 2. (Mylar tape liner).

ometer giving a voltage output which is proportional to displacement. This gage has some advantages over the conventional resistance wire strain gage; it can be simply attached to the tank wall, it can measure high tank strains and if the temperature and thermal contraction coefficient is known for the steel band then thermal contraction of a tank can be calculated.

Test Procedure

The testing of the tanks was divided into three steps:

(1) First, the initial leak rate was established using helium at room temperature and a pressure of 15 pounds per square inch absolute.

(2) The second test consisted of thermally cycling the tank at a constant internal pressure of 1 atmosphere. A thermal cycle consisted of filling the tank with liquid hydrogen, dumping the liquid hydrogen and then warming the tank to room temperature using warm helium. The ability of the liner to withstand repeated thermal stresses was evaluated by examining the leak rate (change of pressure in bell jar).

(3) The third test consisted of pressure cycling the tank at liquid-hydrogen temperature. The pressure increase was obtained by self-pressurization of the liquid hydrogen. For each cycle the pressure was varied from about 15 pounds per square inch absolute (with respect to vacuum in bell jar) to a peak pressure and then back to 15 pounds per square inch absolute. For each subsequent cycle the peak pressure was increased by steps of about 5 pounds per square inch until the liner failed or the ultimate strain of the fiber-glass shell was approached. Again, the leak rate was used to indicate the condition of the tank.

STRUCTURAL ANALYSIS

For the typical liquid-hydrogen tank fabrication and operational procedure assumed for the experimental tanks investigated in this report, there are several physical processes to which the tank structure may be subjected and which must be considered in a design analysis. Some of these are the following:

(1) In order to balance the structural affects of the various components over a wide range of conditions, it may be desirable during fabrication to apply the fiber-glass rovings under tension. Since tension in the winding will produce a compressive load on the liner, the amount of tension applied must not be sufficient to cause the liner to buckle inwardly to produce wrinkles in the liner or to break the adhesive bond between liner and shell when the mandrel is removed.

(2) During pressure testing of a tank at room temperature, the fiber-glass-resin shell is stressed in tension. The liner may be either loaded in compression or tension depending upon the pressure level and the initial compression of the liner due to pretensioning of the fiber-glass roving during tank fabrication. When the pressure level is sufficient to produce tension in the liner, then the liner adhesive joints are subjected to a shearing action. At room temperature, the modulus of elasticity is generally higher for fiber-glass-resin materials than for plastic liner materials. In addition, the ultimate tensile strength of fiber-glass-resin materials is generally higher than the yield strength of plastic liner materials. Thus, if a tank is stressed beyond the yield point of the liner material, the liner will tend to wrinkle when the stress is removed. Wrinkling of the liner with repeated pressure cycles may lead to the development of holes in the liner. Wrinkling may be retarded, however, by the adhesive bond between liner and shell.

(3) During filling of a tank with cryogenic liquid at atmospheric pressure, the liquid and cold gas contacts the liner first, especially near the tank bottom, and thereby sets up radial and longitudinal temperature gradients in the tank wall which are highly transient in nature. When chilled, the liner material and adhesive joints of the liner contract. Shrinkage of the liner tends to reduce any initial compressive load on the liner and if shrinkage is sufficient, then the liner is loaded in tension and adhesive liner joints are loaded in shear. The mechanical load on the liner shifts from compressive to tension when chilled because the liner is attached to the fiber-glass-resin shell which remains at a much higher temperature for a short time. When the liner is loaded in tension, the adhesive bond between liner and fiber-glass-resin shell is also stressed in tension while the fiber-glass-resin shell is loaded in compression. After a time with heat leak into the tank, thermal equilibrium but not uniform temperature conditions are established and the stresses may be somewhat relieved.

(4) When the tank full of cryogenic liquid is pressurized, the liner is pushed out towards the shell producing additional tension in the liner and shear in the liner joints. The tension in the adhesive between liner and shell and the compressive load on the shell is relieved as the pressure increases. When the pressure is increased sufficiently, both liner and shell will be subjected to tension.

(5) Finally, temperature and pressure changes also effect the area around the fill part of the tank by producing tension and shear in the bond lines between liner, fitting, and fiber-glass-resin shell.

Theoretical Considerations

A summary of the present state of the art on design criteria and structural analysis of filament-wound fiber-glass reinforced plastic tanks is presented in reference 6. In

the derivation of analytical expressions for predicting the structural performance, it has in general been necessary to make some simplifying assumptions. The assumptions usually made are as follows:

(1) Only the glass fibers in the structural shell are considered in the analysis, that is, the contribution of any resin liner or sealer materials is assumed negligible.

(2) Stress is proportional to the strain for the fiber glass.

(3) The fibers are straight and continuous.

(4) The resin-to-fiber bond is efficient, so that resin and fiber are strained in equal amount under load.

The validity of using these assumptions has in most cases been verified experimentally. Past analysis, however, have not considered the problem of compatibility of the tank liner with the fiber-glass structural shell when used at liquid-hydrogen temperatures.

The analysis presented herein attempts to describe the behavior of filament-wound shell and liner combinations under pressure loading and thermally induced stresses. The analysis considers only the cylindrical portion of the tank (neglecting the effect of possible discontinuities at the cylinder-dome junction) and to steady-state temperature conditions. It considers both balanced and unbalanced shell designs; the use of several filament-winding angles; and the effect of using a liner bonded to the inside of the tank. Specifically the analysis involves: (1) a two-dimensional load-strain relation for filament-wound structures, (2) a compatibility condition for a liner bonded to the inner shell wall, (3) the pressure-strain relation of the composite cylinder, (4) thermally induced strain in the liner and, (5) strain induced in the liner by winding the fiber-glass shell under tension.

Load-strain relation for filament-wound structures. - For a two-dimensional stress system in an isotropic material, such as a tank liner (the tape liners used were assumed to act as isotropic materials at -423° F), the load-strain relation is the general form of Hooke's law, reference 7:

$$N_{L,\theta} = \frac{E_L t_L}{1-\nu^2}\left(\epsilon_{L,\theta} + \nu\epsilon_{L,Z}\right) \tag{1}$$

$$N_{L,Z} = \frac{E_L t_L}{1-\nu^2}\left(\epsilon_{L,Z} + \nu\epsilon_{L,\theta}\right) \tag{2}$$

where ν is Poisson's ratio for the liner material at -423° F and θ and Z are the orthogonal axies (see fig. 5). Since a filament-wound structure is not isotropic, equations (1) and (2) do not hold for the fiber-glass shell. The load strain relation for a

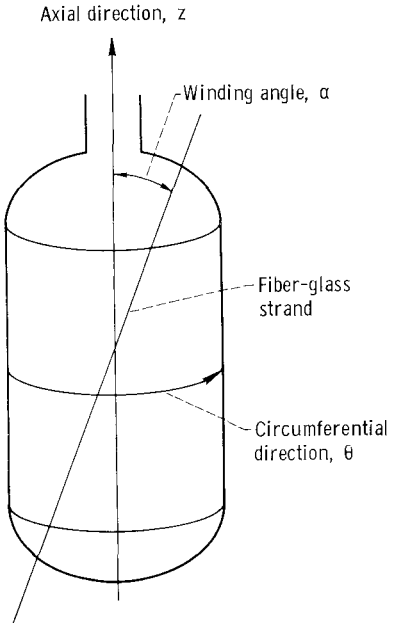

Figure 5. - Definition of coordinates and winding angle.

fiber-glass shell, derived in appendix B, is:

$$N_{S,\theta} = E_g A\left(\epsilon_{S,\theta} K_1 + \epsilon_{S,Z,} K_2\right) \tag{3}$$

$$N_{S,Z} = E_g A\left(\epsilon_{S,Z} K_3 + \epsilon_{s,\theta} K_2\right) \tag{4}$$

where K_1, K_2, and K_3 are constants depending on the densities and angles of the various filament wraps and are

$$K_1 = \sum_i D_i \sin^4\alpha_i$$

$$K_2 = \sum_i D_i \sin^2\alpha_i \cos^2\alpha_i$$

$$K_3 = \sum_i D_i \cos^4\alpha_i$$

where i refers to a particular wrap of filaments of density D all at the same angle α.

Equations (3) and (4) can be used for a fiber-glass shell in the same manner that equations (1) and (2) are used for isotropic materials, such as the liner.

Compatibility of liner and fiber-glass shell. - Upon pressurization, a liner bonded to the inner wall of a fiber-glass filament wound tank will eventually fail in tension, providing the tank does not rupture first. Assuming that the liner remains bonded to the tank wall, the criterion for integrity of the liner is of the form:

$$\text{net liner strain} < \text{ultimate liner strain} \tag{5}$$

where the net liner strain is a combined strain resulting from pressure and thermal stresses and stress due to filament winding tension. It is also desirable to relate the ultimate liner strain to uniaxial tensile test data (the liner is strained biaxially).

In deriving an expression for inequality (5), the following assumptions were made:

(1) Hooke's Law holds for the liner material to the ultimate strain. This is true for many materials at a temperature of -423° F. Some metals are an exception.

(2) The maximum principal stress theory of failure, references 7 and 8, holds for the liner material. This theory is fairly accurate for materials of the type assumed in equation (1) when the signs of the principal stresses are identical (all the stresses are either tensile or compressive), reference 8, page 76, as is the case for the tank liner.

Assuming that the net liner strain ϵ_L can be broken up into the tank strain due to

pressure $\epsilon(P)$, a strain due to thermally induced stresses ϵ_L^T, and a strain due to winding the shell under tension ϵ_L^F, such that $\epsilon_L = \epsilon(P) + \epsilon_L^T - \epsilon_L^F$, yields the following criterion for liner integrity (derived in appendix C):

$$\epsilon(P)_\theta + \nu\epsilon(P)_Z < (1 - \nu^2)\epsilon_{ult} - \epsilon_{L,\theta}^T - \nu\epsilon_{L,Z}^T + \epsilon_{L,\theta}^F + \nu\epsilon_{L,Z}^F \tag{6}$$

$$\epsilon(P)_Z + \nu\epsilon(P)_\theta < (1 - \nu^2)\epsilon_{ult} - \epsilon_{L,Z}^T - \nu\epsilon_{L,\theta}^T + \epsilon_{L,Z}^F + \nu\epsilon_{L,\theta}^F \tag{7}$$

where ϵ_{ult} is the ultimate uniaxial tensile strain of the liner material. To maintain liner integrity, both inequalities must be satisfied. If the functions $\epsilon(P)$ and the values ϵ_L^T and ϵ_L^F are known, inequalities (6) and (7) can be put in the following form:

$$P < \text{constant}$$

$$P < \text{a different constant}$$

The smaller constant will be the pressure at which the liner will theoretically fail in tension.

For the special case of a shell of balanced design and a negligibly thin liner, inequalities (6) and (7) simplify to the single condition:

$$\epsilon(P) < (1 - \nu)\epsilon_{ult} - \epsilon_L^T + \epsilon_L^F \tag{8}$$

The remainder of the analysis is devoted to finding $\epsilon(P)$, ϵ_L^T, and ϵ_L^F.

Pressure-strain relation $\epsilon(P)$. - The basic pressure vessel equation for the liner and fiber-glass shell combination is

$$N_{S,\theta} + N_{L,\theta} = Pr \tag{9}$$

$$N_{S,Z} + N_{L,Z} = \frac{Pr}{2} \tag{10}$$

Since the liner and shell must strain together, ϵ_L and ϵ_S in equations (1) to (4) can both be replaced by the tank strain as a function of pressure $\epsilon(P)$. Then substitution of equations (1) and (3) into equation (9), and equations (2) and (4) into equation (10) results in

$$\left[K_1 + C\right]\epsilon(P)_\theta + \left[K_2 + \nu C\right]\epsilon(P)_Z = \frac{Pr}{E_g A} \tag{11}$$

$$\left[K_3 + C\right]\epsilon(P)_Z + \left[K_2 + \nu C\right]\epsilon(P)_\theta = \frac{Pr}{2E_gA} \tag{12}$$

where

$$C = \frac{E_L t_L}{(1 - \nu^2)E_gA}$$

These are two linear simultaneous equations from which the functions $\epsilon(P)_\theta$ and $\epsilon(P)_Z$ can be calculated. For the special case of a tank of balanced design $\epsilon(P)_\theta = \epsilon(P)_Z$ and a liner of negligible thickness (C = 0), equations (11) and (12) simplify to the same expression:

$$\epsilon(P) = \frac{Pr}{E_gA\sum_i D_i \sin^2\alpha_i} \tag{13}$$

Liner strain due to thermal stress ϵ_L^T. - In general when a free-to-move, homogeneous body is cooled to a certain temperature, it strains by a fixed amount S, the thermal contraction. With this free-to-move body there are no thermal stresses. However if two or more bodies of different materials are fastened together and then cooled, thermal stresses are produced resulting in an additional strain ϵ^T, which in general is different for each of the bodies. The total strain produced by the cooling processes for any one of the bodies is then ϵ^T - S (the negative sign is necessary because S is defined to be positive for a contraction).

For the case of a tank, the shell and liner are bonded together so the total strains of the liner and shell must be identical at every point. Thus,

$$\epsilon^T_{L,\theta} - S_L = \epsilon^T_{S,\theta} - S_S \tag{14}$$

$$\epsilon^T_{L,Z} - S_L = \epsilon^T_{S,Z} - S_S \tag{15}$$

Also, since the shell-liner combination is in a state of mechanical equilibrium,

$$N_{S,\theta} + N_{L,\theta} = 0 \tag{16}$$

$$N_{S,Z} + N_{L,Z} = 0 \tag{17}$$

If ϵ_L and ϵ_S in equations (1) to (4) are replaced by the load producing strains ϵ_L^T and ϵ_S^T, respectively, and ϵ_S^T is eliminated by equations (14) and (15), the substitution of equations (1) and (3) into equation (16), and equations (2) and (4) into equation (17) results in

$$\left[K_1 + C\right]\epsilon_{L,\theta}^T + \left[K_2 + \nu C\right]\epsilon_{L,Z}^T = (S_L - S_S)(K_1 + K_2) \tag{18}$$

$$\left[K_3 + C\right]\epsilon_{L,Z}^T + \left[K_2 + \nu C\right]\epsilon_{L,\theta}^T = (S_L - S_S)(K_3 + K_2) \tag{19}$$

where the bracketed constants on the left hand side are conveniently the same as those in equations (11) and (12).

Equations (18) and (19) are two linear simultaneous equations from which the thermal strains of the liner, $\epsilon_{L,\theta}^T$ and $\epsilon_{L,Z}^T$ can be calculated. For the special case of a liner of negligible thickness ($C \approx 0$), equations (18) and (19) simplify to the same expression:

$$\epsilon_{L,\theta}^T = \epsilon_{L,Z}^T = S_L - S_S \tag{20}$$

Liner strain due to filament winding tension ϵ_L^F. - Winding the fiber-glass shell under tension compresses the liner somewhat when the mandrel is removed. This produces an initial compressive strain ϵ_L^F in the liner. Since the liner and shell are bonded together, the liner and shell strains must be identical at every point.

$$\epsilon_{L,\theta}^F = \epsilon_{S,\theta}^F = \epsilon_\theta^F \tag{21}$$

$$\epsilon_{L,Z}^F = \epsilon_{S,Z}^F = \epsilon_Z^F \tag{22}$$

Also, since the shell and liner are in a state of equilibrium:

$$N_{S,\theta}^0 + \Delta N_{S,\theta} + N_{L,\theta} = 0 \tag{23}$$

$$N_{S,Z}^0 + \Delta N_{S,Z} + N_{L,Z} = 0 \tag{24}$$

where N_S^0 is the initial shell load before the mandrel is removed and N_L and ΔN_S are the liner and additional shell loads produced by the tank strain ϵ^F when the mandrel is removed. In equations (23) and (24) the following substitutions can be made:

For N_L substitute equations (1) and (2) using ϵ_θ^F and ϵ_Z^F.
For ΔN_S substitute equations (3) and (4) using ϵ_θ^F and ϵ_Z^F.
For N_S^0 substitute equations (3) and (4) using

$$\epsilon_\theta = \epsilon_Z = -\frac{F_o}{E_{g,\,RT}A}$$

for the initial shell strain, where F_o is the initial winding tension and $E_{g,\,RT}$ is the room temperature modulus of glass fiber. The term $F_o/E_{g,\,RT}A$ is the initial filament strain which can be considered an initial uniform shell strain (opposite in sign with respect to ϵ^F) producing the initial shell load N_S^0. Equations (23) and (24) then become:

$$\left[K_1 + C\right]\epsilon_\theta^F + \left[K_2 + \nu C\right]\epsilon_Z^F = \frac{F_o}{E_{g,\,RT}A}(K_1 + K_2) \tag{25}$$

$$\left[K_3 + C\right]\epsilon_Z^F + \left[K_2 + \nu C\right]\epsilon_\theta^F = \frac{F_o}{E_{g,\,RT}A}(K_3 + K_2) \tag{26}$$

Equations (25) and (26) are two linear simultaneous equations from which the compressive liner strains ϵ_θ^F and ϵ_Z^F due to winding the shell under tension F_o can be calculated. For the special case of a liner of negligible thickness ($C \approx 0$), equations (25) and (26) simplify to the same expression:

$$\epsilon_Z^F = \epsilon_\theta^F = \frac{F_o}{E_{g,\,RT}A} \tag{27}$$

Application to Test Tanks

If the previously described tanks are at a temperature of -423° F and are pressurized it is assumed that their liners will eventually fail in tension, providing the filament-wound structural shell does not rupture first. Based on the data obtained from the materials study (appendix A), the pressure at which the liner will fail in tension can be calculated using the relations previously derived.

Strain-pressure relation. - First it is necessary to obtain the tank strain as a function of pressure at -423° F. This can be done using equations (11) and (12). These functions work out to be:

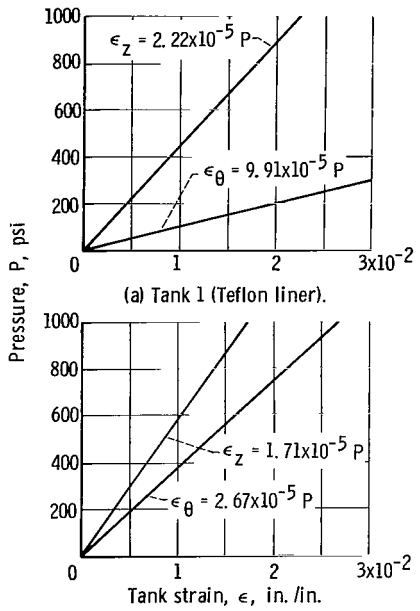

Figure 6. - Calculated tank strain as function of pressure at -423° F for cylindrical parts of tanks 1 and 2.

For tank 1

$$\epsilon(P)_Z = 2.222\times10^{-5}\ P \text{ in./in.}$$

$$\epsilon(P)_\theta = 9.91\times10^{-5}\ P \text{ in./in.}$$

For tank 2

$$\epsilon(P)_Z = 1.71\times10^{-5}\ P \text{ in./in.}$$

$$\epsilon(P)_\theta = 2.67\times10^{-5}\ P \text{ in./in.}$$

These are shown graphically in figure 6. Notice that neither tank is of a balanced design.

The following values were used for the parameters in equations (11) and (12):

$t_L = 0.0133$ in.

$\nu = 0.25$ (ref. 9, p. 69)

$E_g = 12.9\times10^6$ psi at -423° F (appendix A)

$A = 2.08\times10^{-5}$ in.^{2}

For tank 1 (Teflon liner)

$E_L = 0.67\times10^6$ psi at -423° F (appendix A)

$K_1 = 300$ strands/in.

$K_2 = 4.72$ strands/in.

$K_3 = 660.6$ strands/in.

$C = 35.4$ in.$^{-1}$

For tank 2 (Mylar liner)

$E_L = 0.80\times10^6$ psi at -423° F (appendix A)

$K_1 = 1,117$ strands/in.

$K_2 = 138.8$ strands/in.

$K_3 = 705.2$ strands/in.

$C = 42.3$ in.$^{-1}$

Thermal strains of the liner. - Since in general the thermal contraction of the liner material is higher than that of fiber glass, cooling the tanks to -423° F will result in a tensile stress in the liner and a compressive stress in the fiber-glass shell. The amount the liner strains as a result of this stress can be calculated using equations (18) and (19). The thermal strains of the liners work out to be:

For tank 1 (Teflon liner)

$$\epsilon^{T}_{L,\,Z} = 13.3\times10^{-3} \text{ in./in.}$$

$$\epsilon^{T}_{L,\,\theta} = 12.4\times10^{-3} \text{ in./in.}$$

For tank 2 (Mylar liner)

$$\epsilon^{T}_{L,\,Z} = 3.93\times10^{-3} \text{ in./in.}$$

$$\epsilon^{T}_{L,\,\theta} = 4.04\times10^{-3} \text{ in./in.}$$

In this calculation the thermal contraction of the liner (S_L) was taken from the materials study data presented in the appendix A and estimated to be 16×10^{-3} inch per inch for the Teflon liner and 6×10^{-3} inch per inch for the Mylar liner. The thermal contraction of the fiber-glass shell (S_S) was taken as 1.8×10^{-3} inch per inch (appendix A).

Liner strain due to filament winding tension. - A pretension of 1 pound per strand was used when winding tank 2. This tends to put the liner into compression cancelling at least part of the tensile strain of the liner due to thermal contraction. The amount of compressive strain thus produced can be calculated using equations (25) and (26). This works out to be

$$\epsilon^{F}_{Z} = 4.29\times10^{-3} \text{ in./in.}$$

$$\epsilon^{F}_{\theta} = 4.44\times10^{-3} \text{ in./in.}$$

These numbers are somewhat optimistic for two reasons: (1) The mandrel will compress a little bit, effectively lowering the winding tension (F_o), and (2) the adhesive in the joints in the liner may tend to creep or cold flow at ambient temperature thus relieving some of its initial compressive stress.

Application of compatibility condition. - The compatibility condition (inequalities (6) and (7) can now be applied providing that the ultimate uniaxial tensile strain at -423° F of the liner materials (ϵ_{ult}) is known. From the materials study data presented in

appendix A, ϵ_{ult} is about 1.2×10^{-2} inch per inch for the Teflon liner, and 1.4×10^{-2} inch per inch for the Mylar liner.

Using these numbers along with the values for thermal strain and strain due to winding tension, and the pressure-strain function, inequalities (6) and (7) work out to be:

For tank 1:

$$P < -43 \text{ psi, in the } \theta \text{ direction}$$

$$P < -110 \text{ psi, in the Z direction}$$

For tank 2:

$$P < 440 \text{ Psi, } \theta \text{ direction}$$

$$P < 570 \text{ psi, Z direction}$$

This shows that the Teflon liner in tank 1 should not work at all, and the Mylar liner in tank 2 will not fail in tension as long as the internal pressure remains below 440 pounds per square inch. Also as the pressure in tank 2 is increased, the liner will fail first in the θ (circumferential) direction. From figure 6, at a pressure 440 pounds per square inch, the tank 2 strain in the θ direction 1.2 percent, is considerably larger than the strain the Z direction, 0.75 percent.

Domes. - Since the preceeding analysis applies only to the cylindrical part of the tank, the dome shaped ends should also be discussed. This is done in appendix D.

RESULTS AND DISCUSSION

Tank 1 (Teflon Liner)

The initial evaluation of the vessel was made by filling the tank with helium at room temperature and a pressure of 1 atmosphere (with respect to the vacuum in the bell jar). Curve 1, figure 7, shows how the bell-jar pressure varied with time. For a constant leak rate, one would expect this curve to have a constant slope. The nonlinearity is explained by the phenomena known as "out gassing" (the evaporation of contaminants such as water and grease). As the bell-jar pressure increases, the out gassing decreases because the vapor pressure of the contaminate is approached. Therefore only the slope at the right-

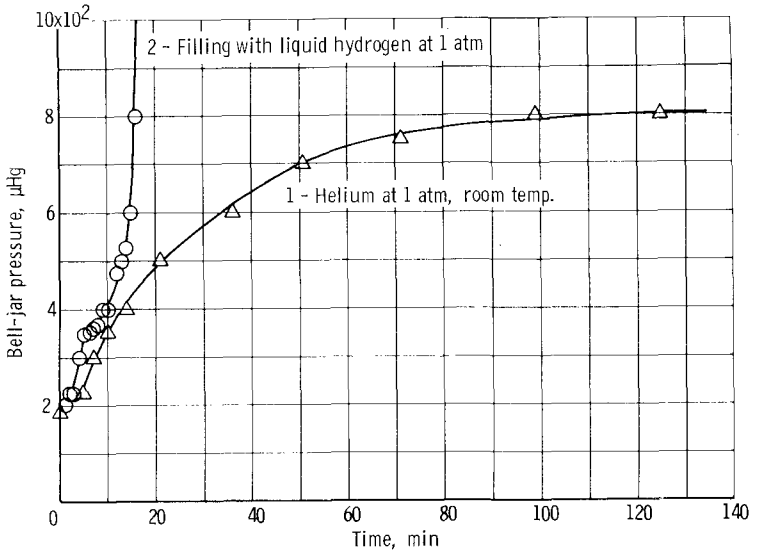

Figure 7. - Tank 1 (Teflon liner) leak rate as indicated by bell-jar pressure as function of time.

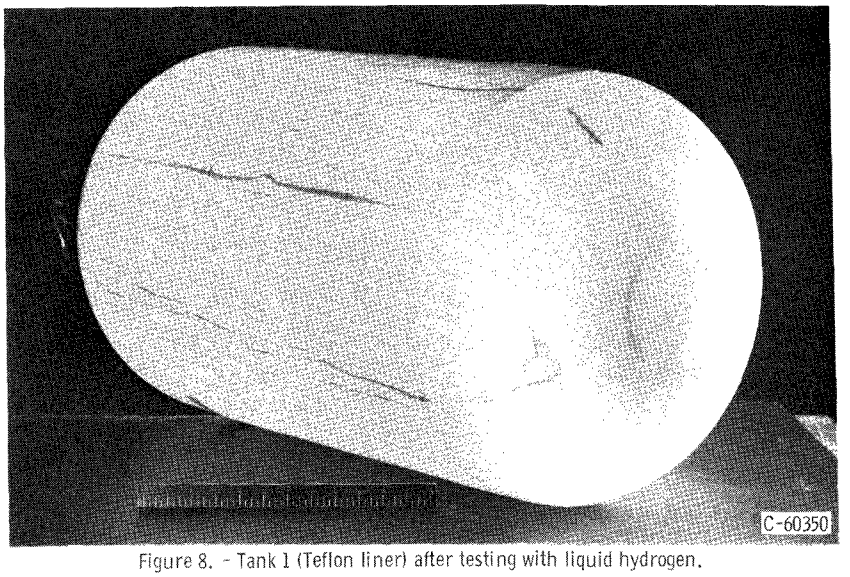

Figure 8. - Tank 1 (Teflon liner) after testing with liquid hydrogen.

hand end of the curve is an indication of the size of the helium leak rate which, in this case, was relatively small.

Upon filling the tank with liquid hydrogen at a pressure of 1 atmosphere, a leak rate of large proportions developed as shown by the slope of curve 2, figure 7.

The tank was removed from the apparatus to discover the cause of the large leak rate. Several areas on the filament-wound shell had a soft or bruised feel to them. The glass fibers were intact but the resin was cracked as if these areas had been bent over a sharp radius. Figure 8 is a photograph of the tank using an internal light source. Certain areas corresponding to the soft or bruised spots previously mentioned, appear dark because of

local delamination of the liner from the tank wall.

From this a hypothesis was drawn that tank 1 had buckled as if by external pressure. However, the conditions of external pressure did not exist. Shell buckling is caused by a compressive stress in the plane of the shell surface. Compressive stresses usually originate from external loads such as pressure. In this case the compressive load may have been caused by thermal stress induced by the difference in thermal contraction between the liner and the filament-wound fiber-glass shell.

Tank 2 (Mylar Liner)

Before testing the tank with liquid hydrogen, an initial leak rate check was made using helium at room temperature and various pressures. Figure 9 is a plot of bell-jar pressure against time for the various tank pressures. As explained before with the Teflon lined tank, the slope of the curves is not constant because of out gassing. Only the slope near the right-hand end of the curves is indicative of the leak rate.

Curve 1, figure 9, is for a tank pressure of 1 atmosphere. The leak rate was found to be 1.85×10^{-3} standard cubic centimeter per second by taking the slope of the curve 1 at a time of 6 hours, and a bell jar pressure of 750 microns of mercury (off scale in

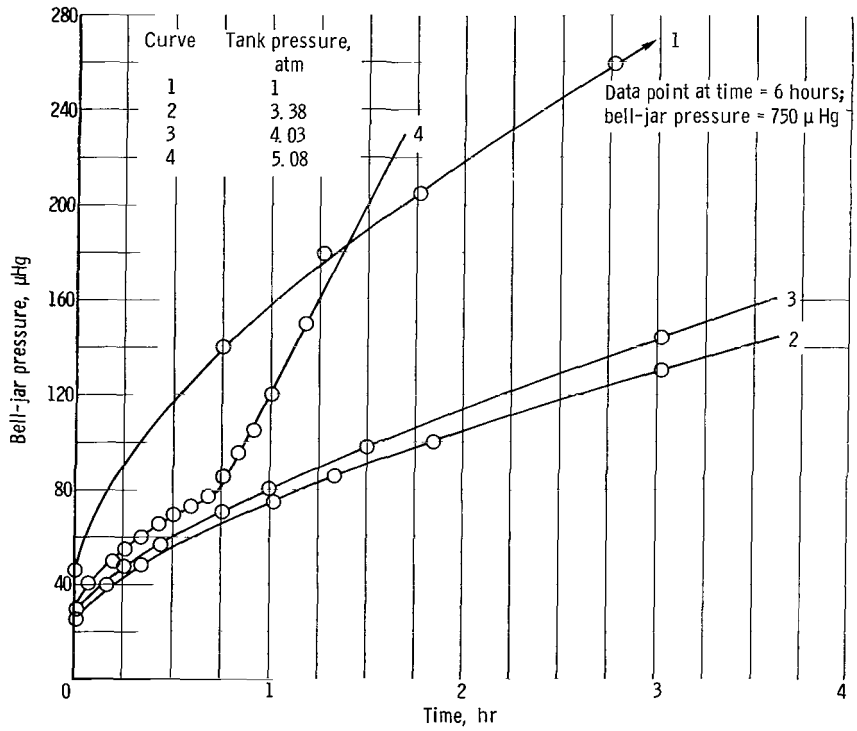

Figure 9. - Tank 2 (Mylar liner) leak rate with room temperature helium as indicated by bell-jar pressure as function of time.

fig. 9). Since this was the first time the outside of the tank was exposed to a vacuum, the curve 1 leak rate was somewhat in error due to a severe amount of out gassing.

From curves 2 and 3, figure 9, the leak rate was found to be 1.82×10^{-3} and 2.19×10^{-3} standard cubic centimeter per second for tank pressures of 3.38 and 4.03 atmospheres, respectively. A calculation showed that the sizes of these leak rates are what would be expected by the permeation of helium through the liner material.

Curve 4, figure 9, is for a tank pressure of 5.08 atmospheres. The sudden change in slope near the 3/4-hour mark was probably caused by the opening of a small hole in the liner due to the high internal pressure. With this hole the leak rate was 1.3×10^{-2} standard cubic centimeter per second at a pressure of 5.08 atmospheres. If this hole had not opened, a calculation shows that the leak rate by the mechanism of permeation would have been 0.3×10^{-2} standard cubic centimeter per second at 5.08 atmospheres. Thus the leak rate remained small even with the suspected hole. From above the leak rate that can be attributed to the hole is 1.0×10^{-2} standard cubic centimeter per second at 5.08 atmospheres and room temperature.

Following the room temperature evaluation, tests were conducted using liquid hydrogen. The tank was put through four temperature cycles from ambient temperature to -423° F at a pressure of 1 atmosphere. Within each cycle, the tank was held for at least 1/2 hour at -423° F (tank containing LH_2). During this hold period, the leak rate was determined. For all four cycles, the tank did not appear to leak, that is, there was no noticeable change in the bell-jar pressure during the 1/2-hour period.

The vacuum gage used had a sensitivity of less than 1 micron in the range of the above measurements. Therefore, the pressure rise in the bell jar must have been less than 1 micron per 1/2 hour. Or a leak rate less than 1.86×10^{-4} standard cubic centimeter per second for each temperature cycle, with liquid hydrogen in the tank at 1 atmosphere pressure. The important thing to note here is that the leak rate did not change from one thermal cycle to the next. Therefore, the repeated thermal stresses were not detrimental to the shell-liner combination. Also judging from the magnitude of the leak rate, the hypothetical hole that opened during the room temperature pressure check must have resealed itself.

After completion of the thermal cycling to -423° F, the tank underwent pressure cycling as shown in figure 10. The tank suddenly began to leak on the pressurization part of the third pressure cycle at a pressure of 32 pounds per square inch absolute.

The tank was then removed from the apparatus and examined. The fiber-glass-resin shell seemed to be in perfect condition. There were no signs of cracking or crazing anywhere.

To find the location of the leak, the tank was pressurized, and a film of soap solution was sprayed over the entire surface of the tank. The only leak was at the very center of

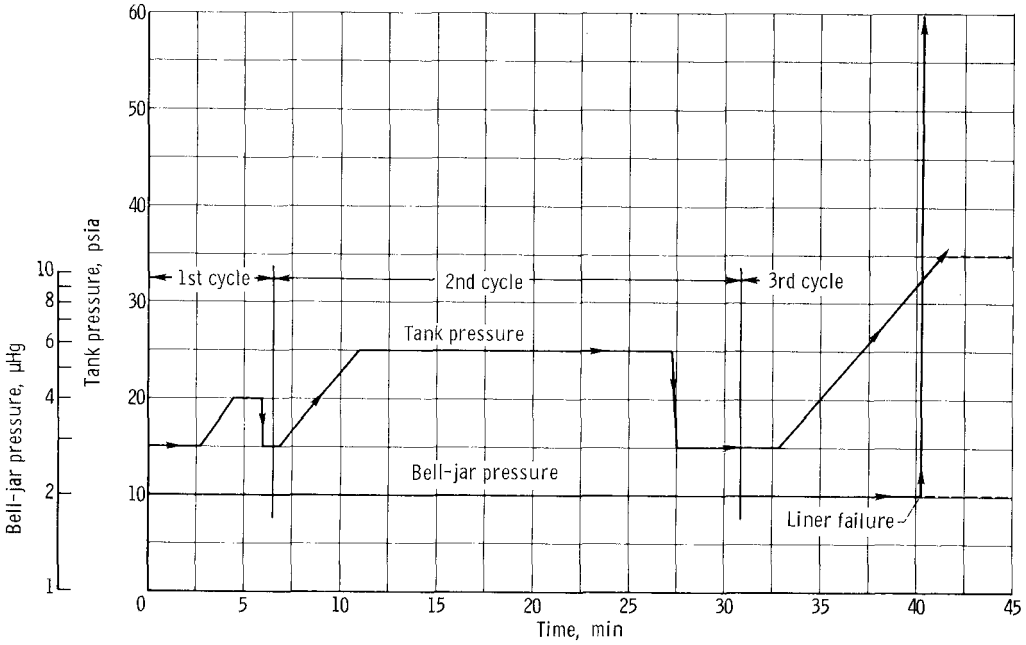

Figure 10. - Tank and bell-jar pressure as function of time for Mylar-lined tank with liquid hydrogen.

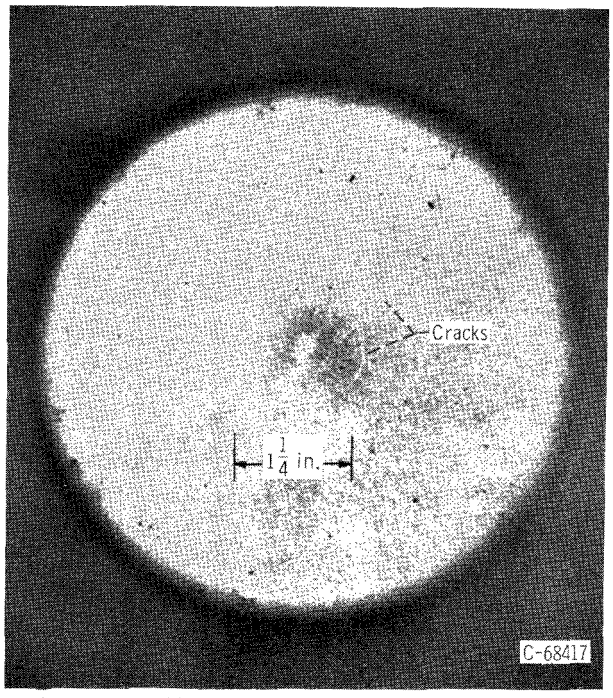

Figure 11. - Inside bottom dome of tank 2 (Mylar lined) after testing with liquid hydrogen.

the lower dome. Figure 11, taken through the neck fitting of the tank, shows cracks in the liner in the area of the failure. Further examination of the liner showed no other cracks or debonding of the liner from the shell.

From the liner strain analysis, it was shown that the liner should not fail until a pressure of approximately 440 pounds per square inch absolute was reached yet it did fail at 32 pounds per square inch absolute. Four possible causes for this premature failure of tank 2 are examined:

(1) The liner strain analysis is in gross error. The only way this analysis can be experimentally verified is by comparing the pressure at which a liner actually fails with what is predicted by theory for many different liners. The liners evaluated in this report did not fail by the mechanism assumed in the derivation of part 2 of the analysis section

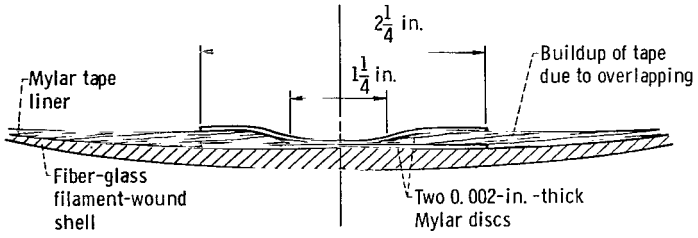

Figure 12. - Cross section of lower dome of filament-wound tank 2 (Mylar liner).

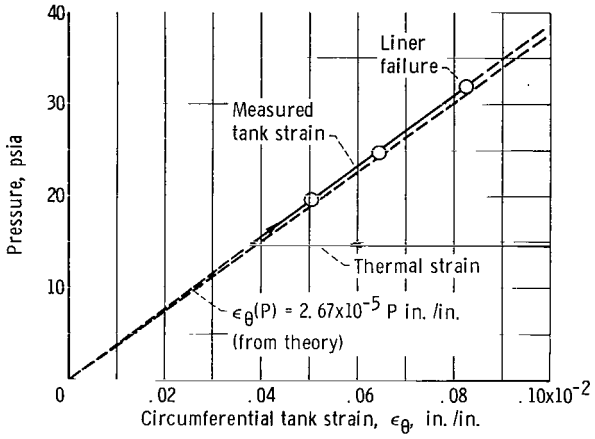

Figure 13. - Tank 2 (Mylar liner) strain as function of pressure at -423° F.

(Compatibility of Liner and Fiber-glass Shell). The analysis assumed a pure tensile failure of a homogeneous liner. The location of the failure in the Myler liner was at a large discontinuity in liner thickness (see fig. 12). Although the overall analysis could not be experimentally verified, a certain part of it could. Figure 13 shows hoop strain ϵ_θ in the cylindrical portion of the tank as a function of pressure both by actual measurement and by the Pressure-Strain Relation (part 3 of the analysis section). The slopes of the two curves are nearly identical. This then substantiates part 3 of the analysis. Since part 3 is based upon part 1 (The Load-Strain Relation For Filament - Wound Structures), part 1 must also be in agreement with the experimental data.

(2) Upon pressurization, the dome contour changed. If the contour changed so the dome tended to flatten near its center, the liner would be put in tension. This would mean that the design contour of the mandrel was not the equilibrium contour of the domes. This, possibly, could be the case since it is difficult to predict the effect of the helical wrap on the dome shape after pressurization.

(3) The premature failure can be attributed to stress concentrations. Since the thickness of the liner changes abruptly (see fig. 12), since most materials are brittle at -423° F, and since the liner was already under a high thermal strain, the slight additional increase of stress due to pressure was enough to cause the liner to fail.

(4) The liner failure at the center of the dome was in an area (the $1\frac{1}{4}$ in. diam area shown in figs. 11 and 12) that was rich in resin. That is, there was a buildup of resin between the two Mylar disks. Since the thermal contraction of the resin is greater than that of Mylar, this would tend to cause a crack to form in the resin around the circumference of the $1\frac{1}{4}$- inch area. Also, because of the differences in thermal contraction, the Mylar, bridging the above mentioned crack, would be put in tension. Upon pres-

surization, then, the liner would fail along this $1\frac{1}{4}$-inch diameter circle. From figure 11, one can see that at least one of the cracks in the liner corresponds to this circle.

Which of the preceding was the actual cause of the failure is unknown. However, for future tanks, it is certainly advisable to design them with minimum discontinuities in the thickness of the liner.

CONCLUDING REMARKS

From this preliminary investigation of bonded plastic tape liners for filament-wound fiber-glass liquid-hydrogen propellant tanks, the following generalizations can be made:

1. Liners bonded to the inner wall of a filament-wound fiber-glass shell can be made that are at least thermally compatable with the shell.

2. The fabrication technique, described in this report, for making a liner out of overlapping tape is feasible.

3. The analytical method of determining a two-dimensional load-strain relation for a filament-wound shell (tank 2) agreed with the experimental data.

4. For thin-walled vessels, shell buckling due to thermal contraction between the liner and the fiber-glass-resin shell can be a problem. However, knowing the physical and mechanical properties of the materials involved, and with proper design, shell buckling can be eliminated.

5. Large discontinuities in the thickness of the liner should be avoided.

6. At -423° F Mylar is more suitable than Teflon for liners bonded to the shell wall.

Since the ultimate strain, at -423° F, of fiber glass is larger than that for Mylar, some techniques to increase the available strain of the liner must be employed. The method of prestressing the glass filaments, used in this program for the Mylar-lined tank, theoretically should help somewhat, but not enough to enable the liner to last until the ultimate strain of the fiber-glass shell is reached. Therefore, an objective of future research should be devising and evaluating means to increase the effective strain or expansion of liners.

Lewis Research Center,
National Aeronautics and Space Administration,
Cleveland, Ohio, September 21, 1965.

APPENDIX A

MATERIALS TESTING

The materials testing program was directed towards obtaining thermal shrinkage data from room temperature to liquid-hydrogen temperature and stress-strain data in the same temperature range for candidate resins, liner (tape resin composites), and fiber-glass-resin composites. Experience with tank number 1 indicated that the plastic film tape liner concept was probably feasible, therefore the materials tests were directed towards this concept. Liner materials tested were Teflon FEP, Mylar, and Kel F-81. The resin formulation Narmco X-292 used in the first tank appeared to be satisfactory, so resin tests were limited to it and a modification designated Narmco X-292A. Flat test specimens of fiber-glass-resin composite representative of two areas of a filament-wound tank (domes and sidewall) were also tested.

Test Specimens

Formulations of X-292 and X-292A resins were cast into flat sheets approximately 1/8-inch thick from which test specimens 1-inch wide by 10-inches long were cut.

Liner test specimens were fabricated from 1-inch-wide by 0.002-inch-thick tapes of the three candidate liner materials: Teflon FEP, Mylar, and Kel F-81. Two layers of tape were wound over a flat mandrel with adjacent tapes in a layer overlapping by 1/4 inch. The overlapping joints and the two layers were bonded together. The liner test specimens were fabricated after test of the resin specimens and as a result of those tests, only resin formula X-292 was used in bonding the liners. After cure of the liner on the mandrel, test specimens 1-inch wide by 10-inches long were cut from the composite in two directions, parallel and perpendicular to the direction of the tapes.

Flat test specimens of fiber-glass-resin composite were made to represent two areas of a tank, the dome where the fibers are approximately unidirectional in the axial direction and the cylindrical portion of the tank where the fibers are oriented biaxially. Two types of specimens were required to represent the cylindrical portion of a tank, one for the axial direction and the other for the circumferential direction. The specimens were cut from composite material made by winding ECG-150-1/0 Fiberglas onto flat mandrels with X-292 resin. The thermal shrinkage specimens were rectangular in shape, 1-inch wide by 10-inches long. The stress-strain specimens were 1-inch wide by 9-inches long with the central portion necked down to a width of 1/2 inch.

Test Apparatus and Procedure

Thermal shrinkage and stress-strain tests were made on an Instron testing machine using a cryostat to cool the specimens to liquid-nitrogen and liquid-hydrogen temperatures. Cooling of the specimens in the cryostat was accomplished by spraying either liquid nitrogen or hydrogen over the entire gage length of the specimen.

For the thermal shrinkage tests of the resins and liner composites the specimens were subjected to a constant load of 0.5 pound and the movement of the testing machine crosshead was measured to the nearest 0.001 inch with a dial indicator as the specimens were cooled down. When movement of the crosshead stopped, indicating temperature equilibrium of specimen had been reached, the specimen was loaded to failure at a crosshead velocity of 0.1 inch per minute.

The thermal shrinkage specimens of the fiber-glass-resin composite were mounted in the testing machine with a 6-inch gage length and were subjected to a 10-pound tensile load during cooldown. The shrinkage was measured in the same manner as for the resin and liner composite specimen. The moduli of the fiber-glass-resin composites were determined with the use of a cryogenic extensometer developed by the contractor.

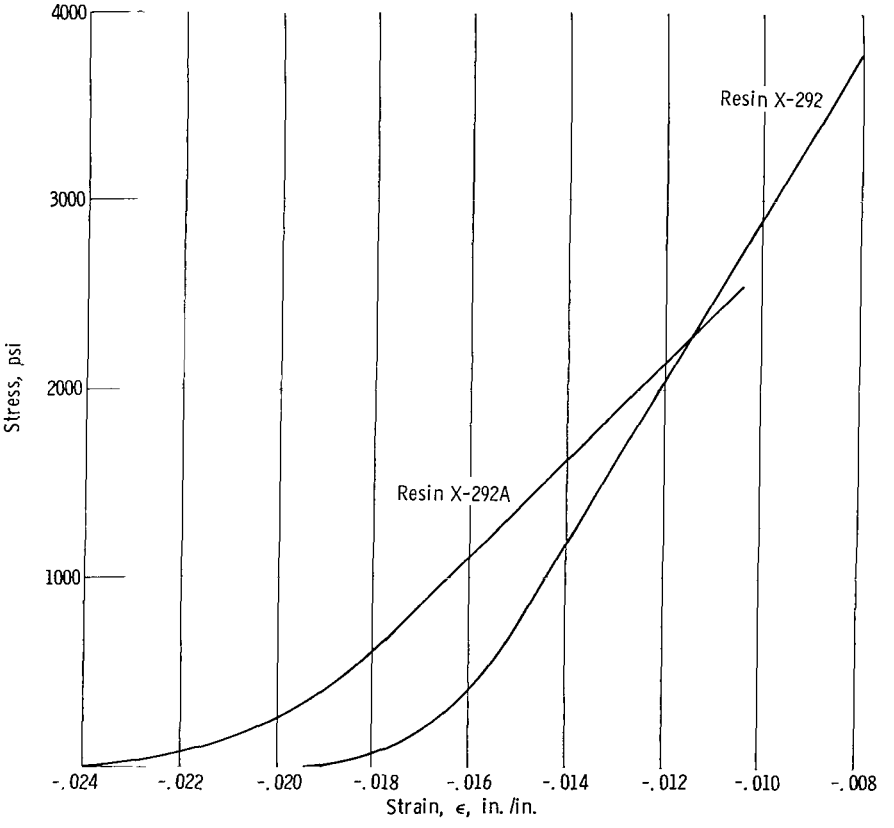

Figure 14. - Resin specimens. Thermal shrinkage from room temperature to 20° K (-423° F) and stress-strain at 20° K.

In addition to the thermal shrinkage and stress-strain data, the resin content of the fiber-glass-resin and liner composites were also determined. The resin content of the fiber-glass-resin composites were determined by comparing the weight of specimens before and after the resin had been burned out of the glass. The resin burning technique could not be used on the liner composites because the liner material would be destroyed also. The resin content of the liner specimens was determined by measuring the thickness of the liner composite. Knowing the thickness of the liner materials, and the number of layers of liner materials in the specimens, the resin thickness was determined and converted to percent of the total volume of the specimen.

Test Results

The thermal shrinkage and stress-strain test results are shown in figures 14 to 19 and in table II. All the results presented are an average of three specimens.

Resin specimens. - The results of the resin test specimens are shown in figure 14. The specimens were assumed to be at zero strain at room temperature. The shrinkage from room temperature to the test temperature, -423° F, was plotted as a negative strain, and this determined the new zero point for plotting the stress-strain curve. Note

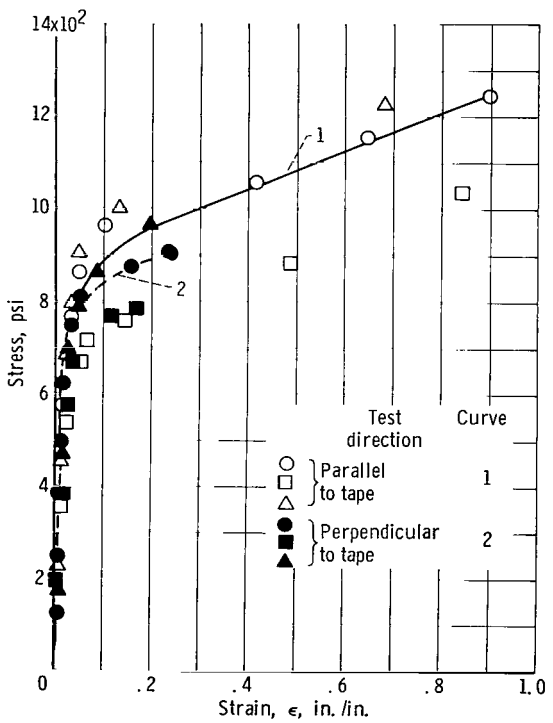

Figure 15. - Stress as function of strain for Teflon tape liner material at room temperature.

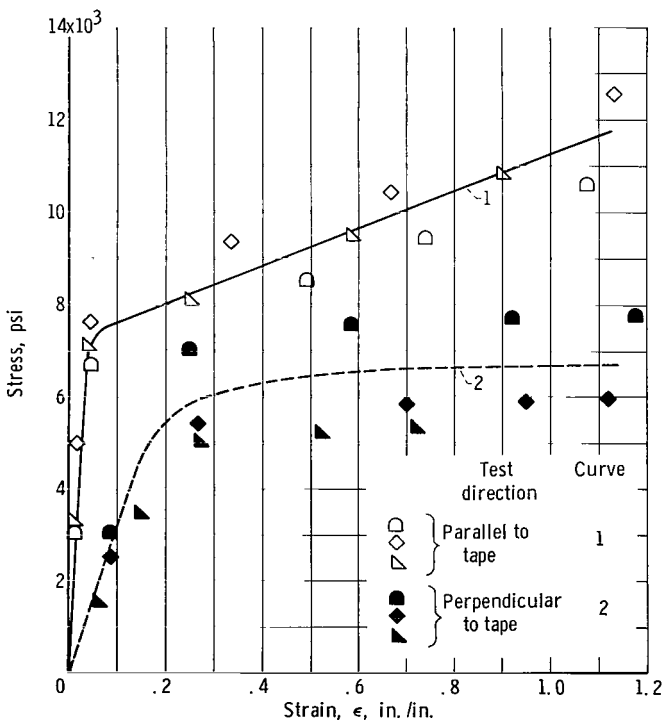

Figure 16. - Stress as function of strain for Mylar tape liner material at room temperature.

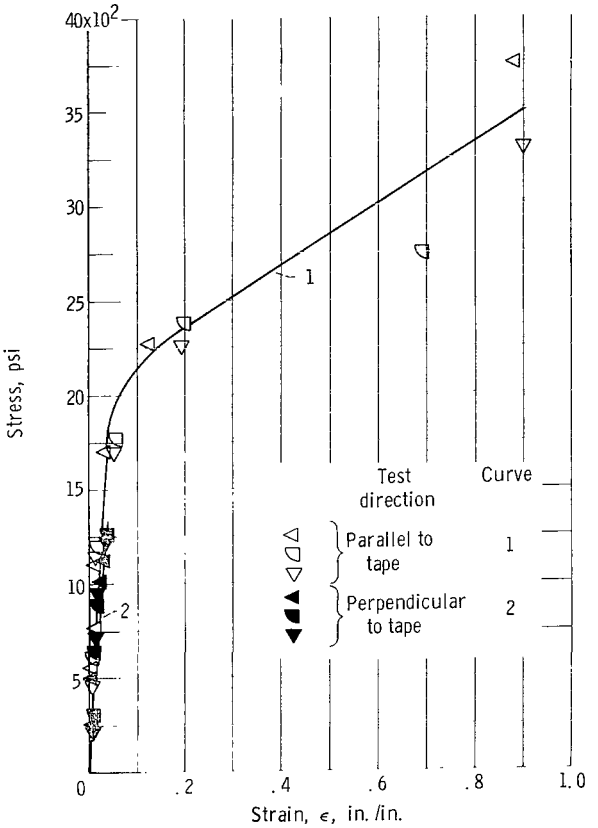

Figure 17. - Stress as function of strain for KEL F-81 tape liner material at room temperature.

that both resins failed at lower elongation than their total shrinkage. Although resin X-292A had a higher elongation than X-292, its shrinkage was considerably higher. Based upon these tests, resin X-292 was chosen for use in bonding the liner specimens.

Liner specimens. - The stress-strain curves for the Teflon FEP, Mylar, and Kel F-81 liner specimens at room temperature are presented in figures 15, 16, and 17 respectively. The shrinkage from room temperature to the test temperature and the stress-strain curves at the test temperature for the Teflon FEP, Mylar, and Kel F-81 liner specimens are shown in figures 18 and 19 for liquid-nitrogen and liquid-hydrogen temperatures, respectively. At -423° F, figure 19, after shrinkage, the Mylar specimens elongate approximately 0.6 to 0.8 percent beyond the room temperature zero strain condition, whereas the Teflon specimens have a negative strain of 0.2 to 0.6 percent at failure. By taking the average slopes of these curves, the moduli E_L are about 0.80×10^6 and 0.67×10^6 pounds per square inch for the Mylar and Teflon liner materials respectively.

The resin content of the liner specimens is as follows:

Material	Percent resin by volume
Teflon FEP	39
Mylar	40
Kel F-81	58

These resin contents are estimated to be accurate to within ±7 percent.

Fiber-glass-resin specimens. - The thermal shrinkage, ultimate stress and moduli of elasticity for the fiber-glass-resin specimens are summarized in table II. When determining the ultimate strength, all specimens failed at the jaws that held them during the tests and not at the necked-down section of the specimen. As a result, the ultimate

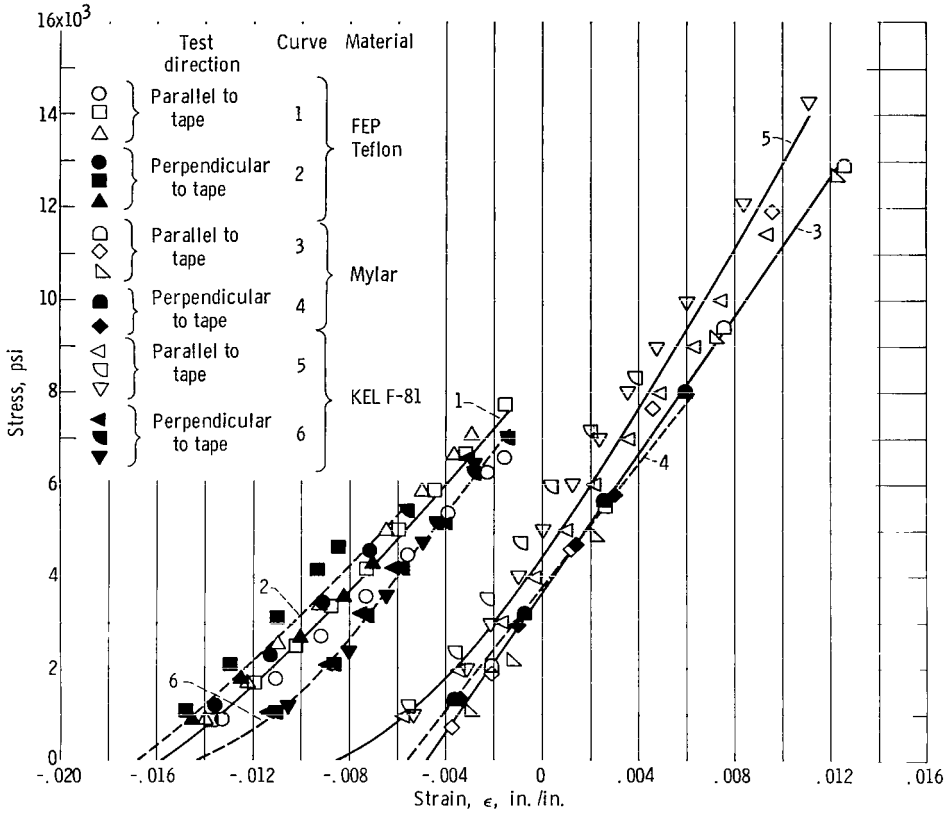

Figure 18. - Thermal shrinkage from room temperature and stress-strain at 76° K (-320° F) for plastic tape liner materials.

strength values are somewhat low. The values of the modulus and ultimate strength are based upon the total cross sectional area of the test section of the specimens. Since in the specimens simulating the cylindrical section of the tank only a portion of the specimen thickness has fiber in the test direction, the values of moduli and ultimate strengths are low. For this reason only the data for the simulated dome specimens (uniaxial fiber direction) were used for thermal contraction and calculating the modulus of glass fiber at -423° F.

In the analytical section of the report it was necessary to know the modulus of pure glass fiber (no resin) at -423° F. The moduli in table II are based on the total cross sectional area of the glass-resin specimen. Furthermore the strand densities of the specimens were unknown. If it is assumed that the glass in the simulated dome specimens carries the entire tensile load (same type of assumption made in the Structural Analysis section), then the change of modulus of the specimen with temperature is due to the change in modulus of the glass within the specimen. In table II the modulus of the dome specimen changes by a factor of 1.23 from room temperature to -423° F. Since the modulus of "E" glass fiber is known to be 10.5×10^6 pounds per square inch (ref. 6)

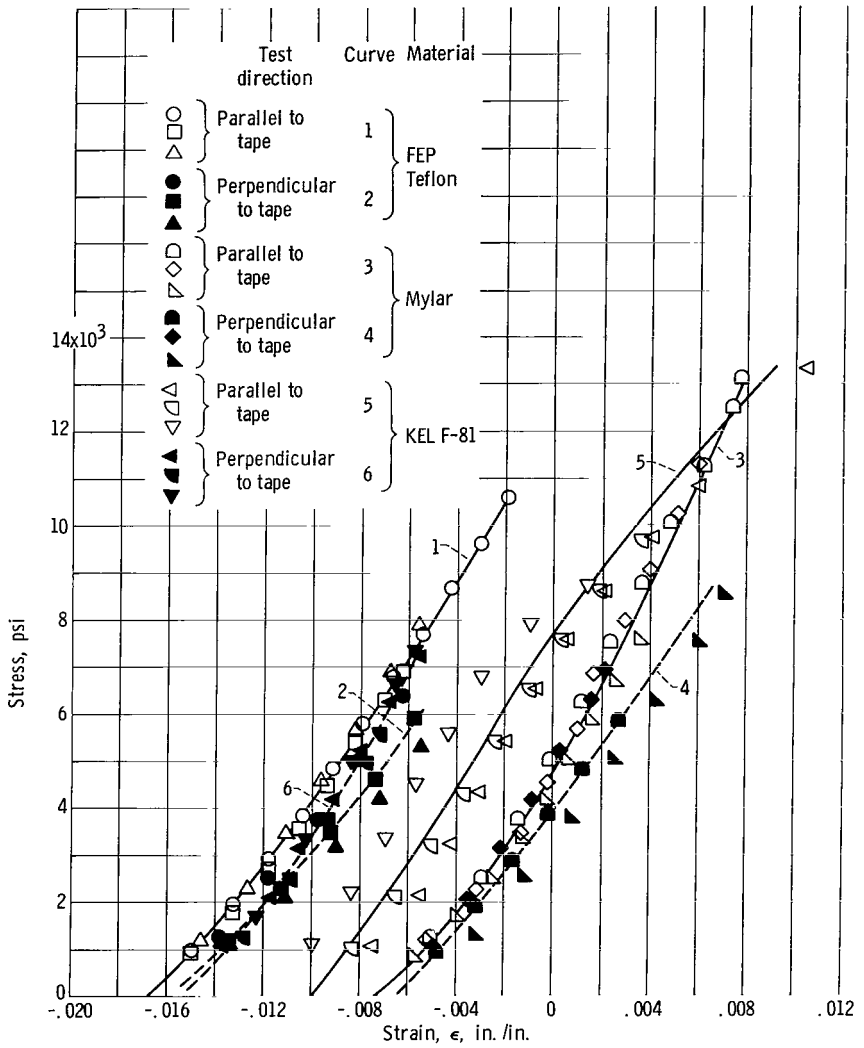

Figure 19. - Thermal shrinkage from room temperature and stress-strain at 20° K (-423° F) for plastic tape liner materials.

at room temperature, the modulus of glass fiber at -423° F can be estimated to be $(1.23)(10.5\times10^6) = 12.9\times10^6$ pounds per square inch.

TABLE II. - TEST RESULTS ON FLAT SHELL SPECIMENS MADE OF FIBER GLASS AND RESIN (NARMCO DATA)

Tank area simulated	Test direction	Resin, percent by weight	Fiber glass, percent by volume	Test temperature								
				Room		76^{o} K(-320^{o} F)			20^{o} K(-423^{o} F)			
				Modulus, psi	Ultimate stress, psi	Shrinkage from room temperature to test temperature, in./in.	Modulus, psi	Ultimate stress, psi	Shrinkage from room temperature to test temperature, in./in.	Modulus, psi	Ultimate stress, psi
				(a)	(a)		(a)	(a)		(a)	(a)
Dome	Axial	33.4	49.5	4.62×10^{6}	54 400	0.0017	5.00×10^{6}	163 400	0.0018	5.69×10^{6}	161 500
Cylinder	Axial	45.0	37.0	1.18×10^{6}	5 700	0.0042	1.36×10^{6}	33 300	0.0050	1.38×10^{6}	29 400
Cylinder	Circum-ferial	32.7	50.0	2.92×10^{6}	22 900	0.0008	3.06×10^{6}	105 600	0.0020	3.19×10^{6}	97 400

[a]Average of three tests.

APPENDIX B

LOAD-STRAIN RELATION FOR FILAMENT-WOUND STRUCTURES

If it is assumed for a fiber-glass-resin composite, that the load carried by the resin is insignificant compared to that carried by the fiber glass, then the load carried by a particular wrap of filaments is given by,

$$N_{S,i} = F_i D_i \tag{B1}$$

where

N_S = fiber-glass shell load, lb/in.

F = glass tension, lb/strand (a strand is a bundle of individual filaments)

The fiber-glass strands used to fabricate the experimental tank of this report were composed of 204 filaments.

D = density of a particular wrap of strands, strands/in.

measured perpendicular to the strand direction α. The subscript i refers to a particular wrap of strands all at the same winding angle α (fig. 5, p. 13).

The components of the glass tension in the θ and Z directions for a particular wrap are:

$$F_{\theta,i} = F_i \sin \alpha_i \tag{B2}$$

and

$$F_{Z,i} = F_i \cos \alpha_i \tag{B3}$$

and the components of the strand density are:

$$D_{\theta,i} = D_i \sin \alpha_i \tag{B4}$$

and

$$D_{Z,i} = D_i \cos \alpha_i \tag{B5}$$

Substitution of equations (B2) to (B5) into equation (B1) gives

$$N_{S,\theta,i} = F_i D_i \sin^2 \alpha_i \tag{B6}$$

$$N_{S,Z,i} = F_i D_i \cos^2 \alpha_i \tag{B7}$$

which are the components of the fiber-glass shell load carried by a particular wrap. The total shell load in the two component directions is the sum of loads carried by all the individual filament wraps; that is,

$$N_{S,\theta} = \sum_i F_i D_i \sin^2 \alpha_i \tag{B8}$$

$$N_{S,Z} = \sum_i F_i D_i \cos^2 \alpha_i \tag{B9}$$

Assuming Hooke's law holds for fiber glass, the glass tension F can be given as:

$$F_i = E_g A \epsilon_i \tag{B10}$$

where

E_g = modulus of elasticity of fiber-glass strands, lb/sq in.

ϵ = strand strain, in./in.

A = cross-sectional area of glass in one strand, $\text{in.}^2/\text{strand}$

Substitution of equation (B10) into equations (B8) and (B9) yields

$$N_{S,\theta} = E_g A \sum_i \epsilon_i D_i \sin^2 \alpha_i \tag{B11}$$

$$N_{S,Z} = E_g A \sum_i \epsilon_i D_i \cos^2 \alpha_i \tag{B12}$$

The strand strain ϵ_i is the same as the shell strain ϵ_S in the α_i direction. The θ and Z components of the shell strain can be related to ϵ_i by geometry using the diagram shown in figure 20. The line $\overline{OA}$ represents a strand on the surface of a tank and $\overline{OA'}$ the same strand after being strained. Now

$$\overline{OA'} = \overline{OA}(1 + \epsilon_i) \tag{B13}$$

$$\overline{OB'} = \overline{OA} \cos\alpha_i(1 + \epsilon_{S,Z}) \tag{B14}$$

$$\overline{OC'} = \overline{OA} \sin\alpha_i(1 + \epsilon_{S,\theta}) \tag{B15}$$

where $\overline{OB'}$ and $\overline{OC'}$ are at right angles to each other and oriented in the Z and θ direactions, respectively. So

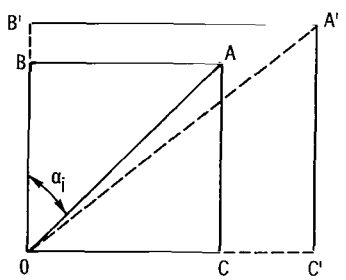

Figure 20. - Planar strain diagram.

$$\left(\overline{OA'}\right)^2 = \left(\overline{OB'}\right)^2 + \left(\overline{OC'}\right)^2 \tag{B16}$$

and therefore

$$(1 + \epsilon_i)^2 = (1 + \epsilon_{S,Z})^2 \cos^2\alpha_i + (1 + \epsilon_{S,\theta})^2 \sin^2\alpha_i \tag{B17}$$

If it is assumed that ϵ is small compared to 1, which is the case for fiber glass, then ϵ^2 can be neglected when it appears along with ϵ in a sum. This assumption reduces equation (B17) to

$$\epsilon_i = \epsilon_{S,\theta} \sin^2\alpha_i + \epsilon_{S,Z} \cos^2\alpha_i \tag{B18}$$

Substitution of equation (B18) into equations (B11) and (B12) gives,

$$N_{S,\theta} = E_g A \sum_i (\epsilon_{S,\theta} \sin^2\alpha_i + \epsilon_{S,Z} \cos^2\alpha_i) D_i \sin^2\alpha_i \tag{B19}$$

$$N_{S,Z} = E_g A \sum_i (\epsilon_{S,\theta} \sin^2\alpha_i + \epsilon_{S,Z} \cos^2\alpha_i) D_i \cos^2\alpha_i \tag{B20}$$

Rearrangement of equations (B19) and (B20) yield:

$$N_{S,\theta} = E_g A \left[\epsilon_{S,\theta} \sum_i D_i \sin^4\alpha_i + \epsilon_{S,Z} \sum_i D_i \sin^2\alpha_i \cos^2\alpha_i\right] \tag{B21}$$

$$N_{S,Z} = E_g A\left[\epsilon_{S,Z} \sum_i D_i \cos^4\alpha_i + \epsilon_{S,\theta} \sum_i D_i \sin^2\alpha_i \cos^2\alpha_i\right] \tag{B22}$$

Since the quantities within the summations are constant for a particular tank, the following constants are defined:

$$K_1 = \sum_i D_i \sin^4\alpha_i \tag{B23}$$

$$K_2 = \sum_i D_i \sin^2\alpha_i \cos^2\alpha_i \tag{B24}$$

$$K_3 = \sum_i D_i \cos^4\alpha_i \tag{B25}$$

Therefore the biaxial load-strain relation for filament-wound structures is:

$$N_{S,\theta} = E_g A(\epsilon_{S,\theta} K_1 + \epsilon_{S,Z} K_2) \tag{B26}$$

$$N_{S,Z} = E_g A(\epsilon_{S,Z} K_3 + \epsilon_{S,\theta} K_2) \tag{B27}$$

Equations (3) and (4) in the structural analysis section are equations (B26) and (B27), respectively.

APPENDIX C

CRITERION FOR LINER INTEGRITY

For Hooke's law holding to the ultimate, the maximum principal stress theory of failure, written for the liner, (refs. 7 and 8) is

$$\sigma_{L,\theta,\max} = \sigma_{ult} \qquad \text{if } \sigma_{L,\theta} > \sigma_{L,Z} \tag{C1}$$

$$\sigma_{L,Z,\max} = \sigma_{ult} \qquad \text{if } \sigma_{L,Z} > \sigma_{L,\theta} \tag{C2}$$

where σ_{ult} is the ultimate uniaxial stress of the liner material at -423° F. For the maximum stress, Hooke's law can be written as:

$$\sigma_{L,\theta,\max} = \frac{E_L}{1-\nu^2}\left(\epsilon_{L,\theta,\max} + \nu\epsilon_{L,Z}\right) \qquad \text{if } \epsilon_{L,\theta} > \epsilon_{L,Z} \tag{C3}$$

$$\sigma_{L,Z,\max} = \frac{E_L}{1-\nu^2}\left(\epsilon_{L,Z,\max} + \nu\epsilon_{L,\theta}\right) \qquad \text{if } \epsilon_{L,Z} > \epsilon_{L,\theta} \tag{C4}$$

Since $\sigma_{ult} = E_L\epsilon_{ult}$ (Hooke's law holding to the ultimate), substitution of equations (C3) and (C4) into equations (C1) and (C2) results in:

$$\epsilon_{L,\theta,\max} = (1-\nu^2)\epsilon_{ult} - \nu\epsilon_{L,Z} \qquad \text{if } \epsilon_{L,\theta} > \epsilon_{L,Z} \tag{C5}$$

$$\epsilon_{L,Z,\max} = (1-\nu^2)\epsilon_{ult} - \nu\epsilon_{L,\theta} \qquad \text{if } \epsilon_{L,Z} > \epsilon_{L,\theta} \tag{C6}$$

Since $\epsilon_L < \epsilon_{L,\max}$ for liner integrity and $\epsilon_L = \epsilon(P) + \epsilon_L^T - \epsilon_L^F$, where $\epsilon(P)$ is the tank strain due to pressure, ϵ_L^T is the liner strain due to thermally induced stresses, and ϵ_L^F is the liner strain due to winding the shell under tension, equations (C5) and (C6) can be put in the form:

$$\epsilon(P)_\theta + \nu\epsilon(P)_Z < (1-\nu^2)\epsilon_{ult} - \epsilon_{L,\theta}^T - \nu\epsilon_{L,Z}^T + \epsilon_{L,\theta}^F + \nu\epsilon_{L,Z}^F \tag{C7}$$

$$\epsilon(P)_Z + \nu\epsilon(P)_\theta < (1 - \nu^2)\epsilon_{ult} - \epsilon^T_{L,Z} - \nu\epsilon^T_{L,\theta} + \epsilon^F_{L,Z} + \nu\epsilon^F_{L,\theta} \quad \text{(C8)}$$

These are two separate conditions, both of which must be satisfied. Inequalities (C7) and (C8) appear as equations (6) and (7) in the section STRUCTURAL ANALYSIS.

APPENDIX D

DOME ENDS

The methods used to calculate dome contours are well known throughout the filament-winding industry (ref. 10). The geometry of the dome surface is adjusted so that the following two requirements are met:

(1) The filament path on the dome surface is also a geodesic path. (A geodesic path is the shortest route between two points on a curved surface.) This is necessary so that the filaments do not tend to slip off the surface during winding and pressurization.

(2) The contour is such that, under pressure loading, a longitudinal strand will exhibit uniform tension in all fibers throughout its length.

These requirements lead to a dome with many desirable characteristics. It is optimum with respect to weight. It has an equilibrium shape; that is, upon pressurization the contour does not change. Because of this, the strain in all directions in the plane of the dome surface is uniform. Also, upon pressurization the strands in the dome are stressed the same amount as the longitudinal strands in the cylindrical portion of the tank (providing the cylindrical portion is composed of longitudinal and 90° circumferential wraps only).

For a balanced shell design, then, the shell strain upon pressurization is the same in all directions and in all parts including the domed-end. A liner in such a shell would be equally strained throughout.

Therefore, the pressure-strain relation previously derived for the cylindrical portion of a filament-wound tank also applies to the entire vessel (including the ends), providing a balanced design is used.

For the case of an unbalanced shell design the situation is complicated. However, there is a simple way of approximating the dome strain. The biaxial dome strain must lie between two limits. One limit is the biaxial strain of the cylindrical portion of the shell. The other limit can be found by fabricating (on paper) another tank. This hypothetical tank must have a dome exactly like the original; however, the cylindrical portion is of balanced design. The other limit, then, is the biaxial strain of the cylindrical portion of this tank.

Applying this to tank 1, one limit of the dome strain due to pressure is the strain of the cylindrical portion (previously calculated and shown in fig. 6), which is

$$\epsilon_Z(P) = 2.22\times10^{-5}\ P \text{ in./in.}$$

$$\epsilon_\theta(P) = 9.91\times10^{-5}\ P \text{ in./in.}$$

The other limit for tank 1, using the hypothetical tank of balanced design, can similarly be calculated by using equations (11) and (12):

$$\epsilon_Z(P) = \epsilon_\theta(P) = 2.36\times10^{-5}\ P \text{ in./in.}$$

Since the actual dome strain must be between these two limits, it must be less than the strain of the cylindrical portion of the real tank. (Although 2.36 is slightly larger than 2.22, 2.36 is much less than 9.91.) Therefore, upon pressurization of tank 1, the liner would fail in the cylindrical portion first (assuming that the liner had not previously failed because of thermal strain).

For tank 2 one limit (the strain of the cylindrical portion previously calculated and shown in fig. 6, p. 18) is

$$\epsilon_Z(P) = 1.71\times10^{-5}\ P \text{ in./in.}$$

$$\epsilon_\theta(P) = 2.67\times10^{-5}\ P \text{ in./in.}$$

The other limit for the hypothetical tank of balanced design works out to be

$$\epsilon_Z(P) = \epsilon_\theta(P) = 2.34\times10^{-5}\ P \text{ in./in.}$$

Although the real tank 2 had a helical wrap that overlapped part of the dome, no helical wrap was considered in the hypothetical tank since the helical wrap did not cover the entire dome.

It is not obvious which of the limits for tank 2 represents the higher biaxial strain. However, the tank pressures at which the liner would be expected to fail in tension can be calculated for each of the limiting strains. For the first limit the pressure required to rupture the liner was already found to be 440 pounds per square inch. For the second limit (using the previously derived condition for liner integrity for a tank of balanced design, inequality (8)), the tank pressure at which the liner should fail works out to be 460 pounds per square inch. This shows that, upon tank pressurization, the liner in tank 2 will fail in tension in the dome at the same or slightly higher pressure (440 to 460 psi) than failure occurs in the cylindrical portion.

REFERENCES

1. Heidelberg, Laurence J.: Evaluation of a Subscale Internally Insulated Fiber-glass Propellant Tank for Liquid Hydrogen. NASA TN D-3068, 1965.
2. Frishmuth, Robert W., Jr.: Investigation of Thin Films as Floating Liners for Fiber-Glass Cryogenic Propellant Tanks. NASA TN D-3205, 1966.
3. Frischmuth, Robert W., Jr.: Experimental Investigation of Glass Flake as a Liner for Fiber-Glass Cryogenic Propellant Tanks. NASA TM X-1193, 1966.
4. Hanson, Morgan P.; Richards, Hadley T.; and Hickel, Robert O.: Preliminary Investigation of Filament-Wound Glass-Reinforced Plastics and Liners for Cryogenic Pressure Vessels. NASA TN D-2741, 1965.
5. Toth, J. M., Jr.; and Barber, J. R.: Structural Properties of Glass-Fiber Filament-Wound Cryogenic Pressure Vessels. Paper Presented at Cryogenic Eng. Conf., Univ. Penn., Aug. 18-21, 1964.
6. Rosato, D. V.; and Grove, C. S., Jr.: Filament Winding. John Wiley & Sons, Inc., 1964.
7. Timoshenko, S.: Strength of Materials. D. Van Nostrand Co., Inc., 1940, p. 473.
8. Seely, F. B.; and Smith, J. O.: Advanced Mechanics of Materials. Second ed., John Wiley & Sons, Inc., 1952, p. 76.
9. Darms, F. J.; Molho, R.; and Chester, B. E.: Improved Filament-Wound Construction for Cylindrical Pressure Vessels. Rept. No. ML-TDR-64-43, Vol. I, Aerojet-General Corp., Mar. 1964.

"The aeronautical and space activities of the United States shall be conducted so as to contribute . . . to the expansion of human knowledge of phenomena in the atmosphere and space. The Administration shall provide for the widest practicable and appropriate dissemination of information concerning its activities and the results thereof."

—NATIONAL AERONAUTICS AND SPACE ACT OF 1958

NASA SCIENTIFIC AND TECHNICAL PUBLICATIONS

TECHNICAL REPORTS: Scientific and technical information considered important, complete, and a lasting contribution to existing knowledge.

TECHNICAL NOTES: Information less broad in scope but nevertheless of importance as a contribution to existing knowledge.

TECHNICAL MEMORANDUMS: Information receiving limited distribution because of preliminary data, security classification, or other reasons.

CONTRACTOR REPORTS: Technical information generated in connection with a NASA contract or grant and released under NASA auspices.

TECHNICAL TRANSLATIONS: Information published in a foreign language considered to merit NASA distribution in English.

TECHNICAL REPRINTS: Information derived from NASA activities and initially published in the form of journal articles.

SPECIAL PUBLICATIONS: Information derived from or of value to NASA activities but not necessarily reporting the results of individual NASA-programmed scientific efforts. Publications include conference proceedings, monographs, data compilations, handbooks, sourcebooks, and special bibliographies.

Details on the availability of these publications may be obtained from:

SCIENTIFIC AND TECHNICAL INFORMATION DIVISION

NATIONAL AERONAUTICS AND SPACE ADMINISTRATION

Washington, D.C. 20546